

**Combined Management of Groundwater Resources and Water Supply  
Systems at Basin Scale under Climate Change**

Giada Felisa<sup>1</sup>, Giulio Panini<sup>1</sup>, Pietro Pedrazzoli<sup>1</sup>, Vittorio Di Federico<sup>2</sup>

<sup>1</sup> IRETI S.p.A., Via Nubi di Magellano 30, 42123 Reggio Emilia, Italy

<sup>2</sup> Department of Civil, Chemical, Environmental and Materials Engineering (DICAM),  
University of Bologna, Viale Risorgimento 2, 40136 Bologna (Italy)

**Contents of this file**

Supplementary Text S1 (S1.1, S1.2, S1.3) to S2 (S2.1, S2.2)

Supplementary Tables S1 to S14

Supplementary Figures S1 to S25

**Introduction**

These Supplementary Materials provide text, figures, and tables that are supplementary to the article.

## Supplementary Text

### S1. Main features of the study area

#### S1.1 Hydrogeological characteristics

The entire area is crossed by Apennine rivers of torrential nature, with maximum monthly flow rates in spring (February, March, April) and autumn (November). In these months, outflow volumes are concentrated in short periods of time; due to the predominantly clayey and poorly permeable nature of the soils forming the mountainous area of the basins, superficial or hypodermic outflows prevail when compared to deep ones. The main rivers crossing the area are depicted in Fig. S1, while Table S1 summarizes their relevant features [RER, 2005; ARPAE, 2020]. Here, the baseflow is computed as the average value between  $Q_{274}$  and  $Q_{355}$  (low flow rates that have been exceeded for 274 and 355 days per year, respectively) during the 2002-2012 decade, derived from the hydrological annals [ARPAE, 2020].

Several geological sections are identified by means of the Emilia Romagna Geoportal [RER, Eni – Agip, 1998; RER, 2020]. The trend of the aquifer limits along Section 35 is showed in Fig. S2.a, while the basal limit of aquifer Group A is depicted in Fig. S2.b, derived by geological sections and Inverse Distance Weighting (IDW) interpolation technique, with QGIS 2.18.

The hydrogeological unit of the Enza river presents different gravel levels with silty-clay intercalations in the southern part, constituting a complex aquifer identifiable as a single-layer system: despite the low permeability, which locally differentiates the layers, the flow exchange between high transmissivity horizons is not prevented. In the northern part of the area, the clay levels delimit a multilayered aquifer, with possible but reduced water exchanges between the layers.

Hydrogeological parameters of the area are obtained from pumping tests performed on the main well fields of the WSS: the average values of transmissivity  $T$ , thickness, and hydraulic

conductivity  $K$  for every well field are reported in Table S2, with indication of the main aquifer group interested by groundwater withdrawals.

### **S1.2 Natural recharge**

A gradual transition from sub-continental temperate climate in the plain and low hill area, to cool temperate type of the high hills and medium mountains is observed in the study area. The distribution of rainfall over the year shows minimum values in summer and winter, and maximum in spring and autumn.

Fig. S5.a-b show respectively the positions of ARPAE rain gauges in the study area, and the average trend of rainfall for the gauges of interest in the 2002-2012 decade [RER, ARPAE, 2019; Antolini et al., 2015]. The values of minimum and maximum temperatures are also obtained from the dataset.

The amount of recharge is estimated by means of a soil classification taken from the regional map [RER, 2018]. Soils are grouped into three macro-categories: fine, medium and coarse. The combination of this classification with the land use map of the Emilia-Romagna Region leads to define waterproof areas.

Rainfall data and annual temperatures for each rain gauge are averaged over the 2002-2012 period, and consequently an average rainfall  $P_m = 771.93$  mm is derived, together with average temperature  $T_m = 14^\circ\text{C}$ . The average annual evapotranspiration  $ETR_m$  is derived by means of Turc equation:

$$ETR_m = \frac{P_m}{\sqrt{0.9 + P_m^2/L^2}} \quad (1)$$

$$L = 300 + 25T_m + 0.05T_m^3 \quad (2)$$

The  $ETR_m$  is estimated as 565.76 mm/year, and the average annual effective precipitation results  $EP_m = P_m - ETR_m = 206.18$  mm/year. Assuming a potential infiltration coefficient of 71%, an estimate of annual average infiltration is obtained as  $I_{m, potential} = 145.4$  mm/year.

The infiltration coefficients, namely the ratios between the flow crossing each type of soil compared to the average flow over the entire area, are estimated in analogies with studies in nearby areas carried out by IRETI and University of Parma: 0.32 for fine soils, 0.72 for medium ones, and 1.82 for coarse soils. Finally, the recharge rate (*RR*) is obtained for every soil:  $1.5 \cdot 10^{-9}$  m/s for fine soils,  $3.5 \cdot 10^{-9}$  m/s for medium ones, and  $8.8 \cdot 10^{-9}$  m/s for coarse soils. The *RRs*, multiplied by the area of each type of soil, lead to an estimate of the average effective infiltration value,  $I_m = 101.31$  mm/year. The distribution of *RRs* within the study area, including impermeable urban areas, is depicted in Fig. S6.

### **S1.3 Climate change in Reggio Emilia province**

Recent studies show that Po plains, and the Emilia-Romagna region, are already undergoing the effects of climate change [Marletto et al., 2010; Pavan et al., 2008; Tomozeiu et al., 2017]. The high frequency of intense precipitation has strong impacts both in urban areas, foothills and adjacent to the rivers, increasing the hydrogeological and hydraulic risk [Westra et al., 2014]. Increasing droughts have negative repercussions on water resources availability, with a foreseeable increased competition for water supply between civil and industrial/agricultural sector [Cacciamani et al., 2007]; in addition, the further groundwater depletion is responsible for reductions in yields and quality of agricultural production [Gorelick et al., 2015].

Since 2009, the Municipality of Reggio Emilia is committed to the climate change issue, implementing actions to mitigate climate-changing emissions. In collaboration with local stakeholders, the Municipality collected numerous data, including climatic and hydrological time series, to build knowledge on the current climate conditions. Subsequently, the National Observatory of Athens carried out an analysis of climate change projections to 2100 [LIFE Urbanproof, 2016a; LIFE Urbanproof, 2016b].

In relation to future projections to 2100, the RCP4.5 scenario adopted by the IPCC [IPCC, 2014] is investigated in this study, according to time series collected in [LIFE Urbanproof, 2016b]. This scenario is representative of a “low-medium” emission case, suggesting that various climate

policies are implemented, e.g. strong reforestation programs, and decrease in the use of cropland and grassland.

Table S5 shows the trends of the most significant variables for RCP4.5 scenarios [LIFE Urbanproof, 2018]. A considerable increase both in average annual maximum and minimum temperature is observed. A significant decrease in total annual rainfall is expected, equal to  $-7.9$  mm/decade, while no significant changes are expected for extreme rainfall. In particular, the effective precipitation is foreseen to decrease of 13% over a 30-year time horizon.

## **S2. Methods: BAU groundwater model**

### **S2.1 Forcing agents in MODFLOW simulation**

The recharge matrix (Recharge package, RCH) is computed according to the methodology described in Text S1.2. The average rainfall is calculated on a quarterly basis, and the average infiltration is obtained through multiplying by the potential infiltration coefficient. Finally, the average infiltration value is distributed according to soil type coefficients (0.32 for fine, 0.72 for medium, 1.82 for coarse), to derive the recharge rate trends for each stress period (SP). The recharge is applied only at the top of the first layer. Fig. S8.a shows the average effective recharge rate (m/s) evaluated in this model, for the entire period of simulation (2002-2012). The impermeable areas have no effective recharge.

The rivers (Stream package, STR) in the active area of the model are previously "hierarchized" by classifying the different branches and their respective tributaries. The complex network of irrigation channels crossing the area is skeletonized into the Enza Canal (Fig. S8.b). The Enza baseflow (branch 1) is lowered from  $0.90 \text{ m}^3/\text{s}$ , registered at Currada station (Table S1), to  $0.81 \text{ m}^3/\text{s}$ , to consider the water surface abstraction located in Cerezzola, further downstream the measuring station. Since no data are available for Enza Canal, the baseflow values of Enza river and Enza Canal are assumed to be equivalent and equal to  $0.4 \text{ m}^3/\text{s}$ . The tributaries 15 and 16 are considered with no flow, as their contribution is not relevant for the purposes of this study.

Moreover, since the Parma and Crostolo rivers are very close to the no-flow boundaries, their baseflows (Table S1) are halved to avoid border effects in the numerical modelling, and consider the symmetrical lack of dispersion of the two rivers. Quarterly time series are adopted to describe the baseflow in every river within the model. Considering  $Q_{av,t}$  as the average value between  $Q_{274,t}$  and  $Q_{355,t}$  in the year of observation  $t$ , for the first and fourth SP of each year, the baseflow is computed as  $Q_{baseflow,t} = 2 \cdot Q_{av,t} - Q_{355,t}$ , while for the second and third SP it is assumed  $Q_{baseflow,t} = Q_{355,t}$ . In case in the year of observation no data are available for  $Q_{274,t}$  and  $Q_{355,t}$ , these are substituted with their average value over the 2002-2012 period (Table S1).

The average water abstractions (Well package, WEL) for each well field are calculated from the annual data provided by IRETI over the 2002-2012 period. The withdrawal is subdivided for each layer of interest, depending on whether the well field falls only in aquifer Group A, only in Group B, or affects both units. A weighted average is adopted according to the hydro-stratigraphic unit involved. Two situations are observed. The first case occurs when the well field crosses the first three layers (Group A). The hydraulic conductivity is equal for all layers, therefore the distribution of the flow rates in each layer  $Q_i$  ( $i = 1, 2, 3$ ) is influenced only by the ratio of the thicknesses between the different layers:

$$Q_1 = \frac{Q_{tot}}{2}; Q_{i=2,3} = \frac{Q_{tot}}{4} \quad (3)$$

where  $Q_{tot}$  is the total flow rate, for each well field. The second situation happens if the well field crosses all four layers (Group A and B,  $i = 1, 2, 3, 4$ ). Here, the transmissivity of the aquifer groups  $T_j$  ( $j = A, B$ ) affects the distribution of the flow rates:

$$Q_i = p_i Q_{tot} \quad (4)$$

with:

$$p_1 = \frac{T_A}{2 \sum_j T_j}; p_{i=2,3} = \frac{p_1}{2}; p_4 = \frac{T_B}{\sum_j T_j} \quad (5)$$

Table S9 shows the value for  $Q_{tot}$ , as average value over the 2002-2012 period, for each well field in the Reggio Emilia area, together with the values of  $Q_i$  and the position in the model. For every SP, the monthly  $Q_{tot}$  is estimated, and consequently  $Q_i$  according to Eq. (3) – (5). The withdrawals from wells in Parma province are evaluated with the same approach.

As irrigation and industrial withdrawals are known at the provincial scale, these are estimated only for the plain areas in the active part of the model, where the withdrawals are concentrated. In particular, the average value of irrigation withdrawals (Table S3), i.e. 33.7 Mm<sup>3</sup>/year, is multiplied by the ratio between the active area of the model and the whole plain area of Reggio Emilia Province (about 50% of the area of the entire province), resulting in 16.9 Mm<sup>3</sup>/year. The same methodology is applied to derive the industrial withdrawals for the area of interest, considering that at the provincial scale it is estimated as 19 Mm<sup>3</sup>/year, leading to 8.4 Mm<sup>3</sup>/year. The total  $Q_{irr\_ind}$ , i.e. 25.3 Mm<sup>3</sup>/year, is equally divided among the four layers. The irrigation and industrial withdrawals are then evenly distributed amongst all cells over the whole active area. To avoid the presence of dry cells during the simulation, these withdrawals are distributed assuming that: i) from line 12 to 62 of the model, the withdrawals involve only the first and second layer (3990 cells for each layer); ii) from line 63 to 82, the third layer (1900 cells); iii) from line 83, the fourth layer (2142 cells). This distribution is represented in Table S10. In addition, irrigation withdrawals are concentrated over the second and third SP period of each year, when irrigation activity is usually more intensive, while the distribution is taken as uniform throughout the year for industrial abstractions. Fig. S8.c – d provide respectively the irrigation and industrial withdrawals trend for each SP (S8.c), the civil withdrawals trend from the well fields of Reggio Emilia Province (S8.d), and the location of water withdrawals in the model.

Finally, multiple channels and “fontanili” (springs) are present in the study area. The main two “fontanili”, i.e. Laghi di Gruma and Fontanili di Corte Valle Re, are modelled as drains (Drain package, DRN), assuming a head equal to DEM - 1 m for both. These are modelled considering the conductance  $C$  (m<sup>2</sup>/s), evaluated as  $C = k_{vert} \cdot A/L$ , where  $A$  is the area of the object, and  $L$  is the length of the boundary condition in the cell assumed unitary. The location of the drains inserted in the model is shown in Fig. S8.f.

## **S2.2 Calibration and validation**

Model calibration for BAU groundwater model is performed against the levels measured in monitoring wells belonging to the water company and to a private network (Fig. S9.a), for a total of over 1,400 data in the 2002-2012 decade. A first calibration phase is performed in stationary mode to infer the vertical hydraulic conductivity  $k_{vert}$ , while the simulation in transient mode allows to determine the aquifer specific storage  $S_s$ . Transient simulations are performed with a quarterly discretization, i.e. a 3-month time step.

Comparing the levels observed in the monitoring and private wells with those predicted by the transient simulation, a high coefficient of determination  $R^2$  is observed (Fig. S9.b). Moreover, the time series of the observed and predicted levels exhibit the same trend as shown in Fig. S9.c-d, for the 2002-2012 decade: here, the observed levels of Roncocesi and Quercioli wells, derived by the average values of the two wells RON011-RON018 and QUE009-QUE010 respectively, are compared against the predicted levels of transient simulation. It should be noted that levels observed at the wells are punctual data, while the values returned from the simulation are averaged over the cell, whose dimension (square cells of 250 m) depends on the spatial discretization. However, the tendency observed in single wells towards an increase in level is preserved also at the scale of the numerical simulations.

A validation is also performed to evaluate the accuracy of the BAU model. To achieve this goal, the previous analysis over 2002-2012 decade is extended from 2012 to 2015. We consider the same monitoring wells as for calibration, with levels observed in the period of interest, and

adopt withdrawals data collected from IRETI, rainfall and temperature time series as described in Text S1.2 [RER, ARPAE, 2019], and baseflows derived from the annex and modulated with the same approach in Text S2.1.

Results of validation are depicted in Fig. S9.b-d. It is possible to observe that these are clustered again around a 45° regression line, with negligible spreading: this denotes that the model is robust and provides a very good performance in reproducing the available observations.

## References

- Regione Emilia-Romagna (2005). Piano di Tutela delle Acque. Approvato con Delibera dell'Assemblea Legislativa della Regione Emilia-Romagna n. 40 del 21 dicembre 2005
- ARPAE Emilia-Romagna (2020) Annali Idrologici – Parte II. Available online: [https://www.arpae.it/documenti.asp?parolachiave=sim\\_annali&cerca=si&idlivello=64](https://www.arpae.it/documenti.asp?parolachiave=sim_annali&cerca=si&idlivello=64) (accessed on 24 May 2020)
- Regione Emilia-Romagna, Eni – Agip (1998). Riserve idriche sotterranee della Regione Emilia-Romagna; G. Di Dio, S.E.L.C.A. (Firenze)
- Regione Emilia-Romagna (2020). Sezioni geologiche e prove geognostiche della pianura emiliano romagnola. Available online: [https://geo.regione.emilia-romagna.it/cartografia\\_sgss/](https://geo.regione.emilia-romagna.it/cartografia_sgss/) (accessed on 24 May 2020)
- Regione Emilia-Romagna, ARPAE (2019). Analisi climatica giornaliera ERG5\_Eraclito. Available online: <https://dati.arpae.it/dataset/erg5-eraclito> (accessed on 31 May 2020).
- G. Antolini, L. Auteri, V. Pavan, F. Tomei, R. Tomozeiu, V. Marletto (2015). A daily high-resolution gridded climatic data set for Emilia-Romagna, Italy, during 1961-2010. *International Journal of Climatology* 08/2015; doi:10.1002/joc.4473
- Regione Emilia-Romagna (2018) Carta dei suoli – Pianura, basso e medio Appennino emiliano-romagnolo, scala 1:50.000 - Edizione 2018. Available online: <https://datacatalog.regione.emilia-romagna.it/catalogCTA/dataset/carta-dei-suoli-scala-1-50-000> (accessed on 31 May 2020)

- Marletto V., G. Antolini, F. Tomei, V. Pavan, R. Tomozeiu (2010). Atlante idroclimatico dell'Emilia-Romagna 1961-2008. Arpa Emilia-Romagna, ISBN 88-87854-24-6.
- V. Pavan, R. Tomozeiu, C. Cacciamani, M. Di Lorenzo (2008). Daily precipitation observations over Emilia-Romagna: mean values and extremes, *International Journal of Climatology*, vol. 28, no. 15, pp. 2065–2079.
- Tomozeiu R., Pasqui M., Quaresima S. (2017). Future changes of air temperature over Italian areas: statistical downscaling technique applied to 2021-2050 and 2071-2100 periods. *Meteorology and Atmospheric Physics*, doi.org/10.1007/s00703-017-0536-7.
- Westra, S., H. Fowler, J. Evans, L. Alexander, P. Berg, F. Johnson, E. Kendon, G. Lenderink, and N. Roberts (2014). Future changes to the intensity and frequency of short-duration extreme rainfall, *Rev. Geophys.*, 52, 522–555, doi:10.1002/2014RG000464.
- C. Cacciamani, A. Morgillo, S. Marchesi, and V. Pavan (2007). Monitoring and forecasting drought on a regional scale: Emilia-Romagna region, *Water Science and Technology Library*, vol. 62, part 1, pp. 29–48.
- Gorelick, S. M., and C. Zheng (2015). Global change and the groundwater management challenge, *Water Resour. Res.*, 51, 3031–3051, doi:10.1002/2014WR016825.
- LIFE Urbanproof (2016a) Deliverable C.1.1. Investigation of current climate change impacts and vulnerability & recording of the socio-economic profile.
- LIFE Urbanproof (2016b) Deliverable C.2: Report on historical data trends and climate change projections for the greater urban areas of interest.
- IPCC (2014). *Climate Change 2014: Synthesis Report. Contribution of Working Groups I, II and III to the Fifth Assessment Report of the Intergovernmental Panel on Climate Change* [Core Writing Team, R.K. Pachauri and L.A. Meyer (eds.)]. IPCC, Geneva, Switzerland, 151 pp.
- LIFE Urbanproof (2018). Cambiamenti climatici a Reggio Emilia. Analisi dei dati storici e proiezioni al 2100. Available online:  
<https://www.comune.re.it/retcevica/urp/retecivi.nsf/PESDocumentID/23A9BECB5AF04F47C1258330003B942A?opendocument> (accessed on 21 June 2020)

## Supplementary Tables

**Table S1** Features of the main rivers in the study area

River	Basin (km <sup>2</sup> )	Altitude (m)	Baseflow (m <sup>3</sup> /s)
Enza	430	231	0.90
Parma	111	529	0.38
Crostolo	86	126	0.19
Rio Zolle	5	200	0.01
Masdone	12	200	0.01
Termina	65	200	0.10

**Table S2** Hydrogeological parameters obtained from pumping tests in the main well field.

Well field	$T$ (m <sup>2</sup> /s)	Thickness (m)	$K$ (m/s)	Aquifer Group
Bellarosa	3.56E-02	129	2.76E-04	A
S. Ilario	1.70E-02	108	1.57E-04	A
Caprara	2.27E-02	180	1.26E-04	A
Roncocesi	1.91E-02	195	9.81E-05	A
Caneparini	1.00E-02	107	9.35E-05	A
Case Corti	2.20E-02	104	2.12E-04	A
Quercioli (1)	9.00E-03	111	8.14E-05	A
Quercioli (2)	1.00E-04	50	2.00E-06	B
Mangalana	3.90E-03	21	1.86E-04	B
Aiola	6.62E-03	56	1.18E-04	B
Malamassata	5.10E-03	53	9.62E-05	B

**Table S3** Irrigation withdrawals (Mm<sup>3</sup>/y) in Reggio Emilia Province, from 2002 to 2012

	2002	2003	2004	2005	2006	2007	2008	2009	2010	2011
RE	21.5	57	27.1	51.4	35.9	34.2	23.7	31.3	18.9	36

**Table S4** Withdrawals (Mm<sup>3</sup>/y) for different uses from Enza alluvial fan, in 2010

ID	Groundwater body	Civil	Industrial	Irrigation	Zootechnical
IT080090ER-DQ1-CL	Enza phreatic aq.	2.6	1.2	8.6	0.5
IT080370ER-DQ2-CCS	Enza upper confined aq.	8.7	0.4	3.4	0.4
IT082370ER-DQ2-CCI	Enza lower confined aq.	16.7	0.3	4.8	0.1

**Table S5** Projections to 2100 of climate indicators for Reggio Emilia (RCP4.5 scenario)

Indicators	RCP4.5
Average annual Tmax	+ 0.2°C/decade
Average annual Tmin	+ 0.2°C/decade
Extreme Tmax	Tmax >30°C (34 more days) Tmax >35°C (32 more days) Tmax >40°C (11 more days)
Extreme Tmin (>20°C)	40 more days
Annual rainfall	-7.9 mm/decade

**Table S6** Vertical discretization of the model

Layer	Group	Top layer	Bottom layer
1	A0 + A1	Digital Elevation Model (DEM)	DEM – (Thickness Group A)/2
2	A2	Bottom layer 1	Bottom layer 1 - (Thickness Group A)/4
3	A3 + A4	Bottom layer 2	Bottom layer 2 - (Thickness Group A)/4
4	B	Bottom layer 3	Bottom Group B

**Table S7** Summary of stress packages and parameters in groundwater model

Forcers – Stress package	Parameters
Rivers – STREAM (STR)	Conductance (m <sup>2</sup> /s), Hydraulic head (m), Baseflow (m <sup>3</sup> /s)
“Fontanili” (springs) – DRAIN (DRN)	Conductance per unit length (m <sup>2</sup> /s), Hydraulic head (m)
Recharge – RECHARGE (RCH)	Recharge rate (m/s)
Withdrawals – WELL (WEL)	Pumping rate (m <sup>3</sup> /s) for each layer

**Table S8** Features of STR package

Parameters	Values
Head Stream (m)	Digital Elevation Model (DEM)
Streambed bottom (m)	DEM – 2 m
Streambed top (m)	DEM – 1 m
Outflow segment	Branch into which more tributaries converge Enza river (branch 1) 0.4 m <sup>3</sup> /s; Parma river (branch 8) 0.19 m <sup>3</sup> /s; Crostolo river (branch 12) 0.10 m <sup>3</sup> /s; Rio Zolle (branch 6), Masdone (branch 4), and Quaresimo (branch 10) 0.01 m <sup>3</sup> /s; Termina (branch 2) 0.10 m <sup>3</sup> /s; Modolena (branch 9) 0.05 m <sup>3</sup> /s; Enza Canal: (branch 14) 0.4 m <sup>3</sup> /s, (branches 15 and 16) 0 m <sup>3</sup> /s
Flow (m <sup>3</sup> /s)	
Conductance (m <sup>2</sup> /s)	$k_{vert}$ with option "calculated per unit of length or area"

**Table S9** Average withdrawals (m<sup>3</sup>/s) of the well fields in Reggio Emilia Province

Well field	Layer	Row	Column	$Q_i$ (m <sup>3</sup> /s)	$Q_{tot}$ (m <sup>3</sup> /s)
Bellarosa	1	55	65	1.15E-02	0.0230
	2	55	65	5.75E-03	
	3	55	65	5.75E-03	
Gazzaro	1	57	54	4.17E-03	0.009
	2	57	54	2.09E-03	
	3	57	54	2.09E-03	
	4	57	54	6.53E-04	
Cabina Gas	1	54	54	2.30E-04	0.0005
	2	54	54	1.15E-04	
	3	54	54	1.15E-04	
Pensile	4	52	55	6.00E-03	0.006
Caprara	1	47	70	5.00E-02	0.1
	2	47	70	2.50E-02	
	3	47	70	2.50E-02	
Roncocesi	1	61	93	1.08E-01	0.2160
	2	61	93	5.40E-02	
	3	61	93	5.40E-02	

Well field	Layer	Row	Column	$Q_i$ (m <sup>3</sup> /s)	$Q_{tot}$ (m <sup>3</sup> /s)
Quercioli	1	69	77	1.19E-01	0.2720
	2	69	77	5.95E-02	
	3	69	77	5.95E-02	
	4	69	77	3.42E-02	
Case Corti	1	75	88	2.97E-02	0.068
	2	75	88	1.49E-02	
	3	75	88	1.49E-02	
	4	75	88	8.55E-03	
S.Ilario nuovo	1	57	59	6.25E-02	0.125
	2	57	59	3.13E-02	
	3	57	59	3.13E-02	
Caneparini	1	76	85	1.75E-02	0.04
	2	76	85	8.74E-03	
	3	76	85	8.74E-03	
	4	76	85	5.03E-03	
Aiola	4	71	65	3.60E-02	0.036
Malamassata	4	90	61	2.00E-03	0.02
Mangalana	4	101	73	1.40E-02	0.014
Rubbiano	4	102	82	8.00E-03	0.008

**Table S10** Average irrigation and industrial withdrawals  $Q_{irr\_ind}$  (m<sup>3</sup>/s) in the active area, by layer and cells

Layer	$Q_{irr\_ind,i}$ (m <sup>3</sup> /s)	Cells (n°)	$Q_{cell,i}$ (m <sup>3</sup> /s)
1	0.2	3,990	5.02E-05
2	0.2	3,990	5.02E-05
3	0.2	1,900	1.05E-04
4	0.2	2,142	9.34E-05

**Table S11** Average baseflows in ST1 over the 30-year time horizon (2020-2050)

Rivers	Baseflow RCP4.5 (m <sup>3</sup> /s)
Parma	0.360
Enza	0.383
Crostolo	0.176
Termina	0.095
Masdone	0.010
Rio Zolle	0.010
Modolena	0.048
Quaresimo	0.010
Canale Enza	0.383

**Table S12** Flow max amount (MI/day) extracted from well fields

Well fields	Flow Max Amount (MI/day)
Pump_Bellarosa	3.36
Pump_Gazzaro	1.04
Pump_CabinaGas	0.14

Well fields	Flow Max Amount (MI/day)
Pump_Pensile	1.90
Pump_Caprara	9.57
Pump_Roncocesi	23.84
Pump_Quercioli	31.91
Pump_Case Corti	10.76
Pump_S. Ilario Nuovo	15.13
Pump_Caneparini	5.15
Pump_Aiola	3.75
Pump_Malamassata	1.23
Pump_Mangalana	3.40
Pump_Rubbianino	1.81
Pump_Parma	35.22

**Table S13** Water deficit (Mm<sup>3</sup>) as a function of Surplus demand for different RV2 volumes and BAURV2 and ST2 scenarios

RV2 Volume (Mm <sup>3</sup> )	Deficit (Mm <sup>3</sup> )							
	Surplus		Surplus + 25%		Surplus + 50%		Surplus + 100%	
	BAURV2	ST2	BAURV2	ST2	BAURV2	ST2	BAURV2	ST2
10	11.2	17.0	25.9	36.7	48.4	62.3	104.4	131.5
15	3.3	5.7	8.6	14.1	20.9	29.9	64.3	83.7
20	0	0.7	3.6	6.5	9.3	13.5	33.6	48.9
25	0	0	0	1.5	4.3	7.2	18.7	25.0
30	0	0	0	0	0	2.2	10.9	14.3
35	0	0	0	0	0	0	5.9	8.8
40	0	0	0	0	0	0	0.9	3.8
45	0	0	0	0	0	0	0	0
50	0	0	0	0	0	0	0	0

**Table S14** Number of days in a decade when the Enza MVF is released from the RV2 reservoir, and corresponding percentage (BAURV2 and ST2)

	MVF days			
	Surplus	Surplus + 25%	Surplus + 50%	Surplus + 100%
BAURV2	1,321 (36.2%)	1,543 (42.3%)	1,686 (46.2%)	2,040 (55.9%)
ST2	1,554 (42.6%)	1,756 (48.1%)	1,948 (53.4%)	2,251 (61.7%)



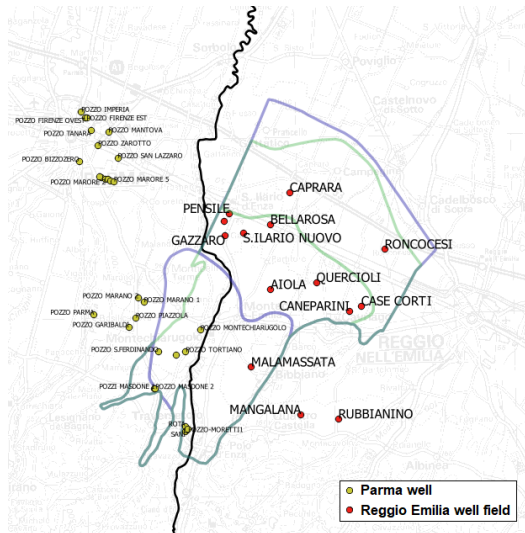


Fig. S3 Location of Reggio Emilia well fields and Parma wells

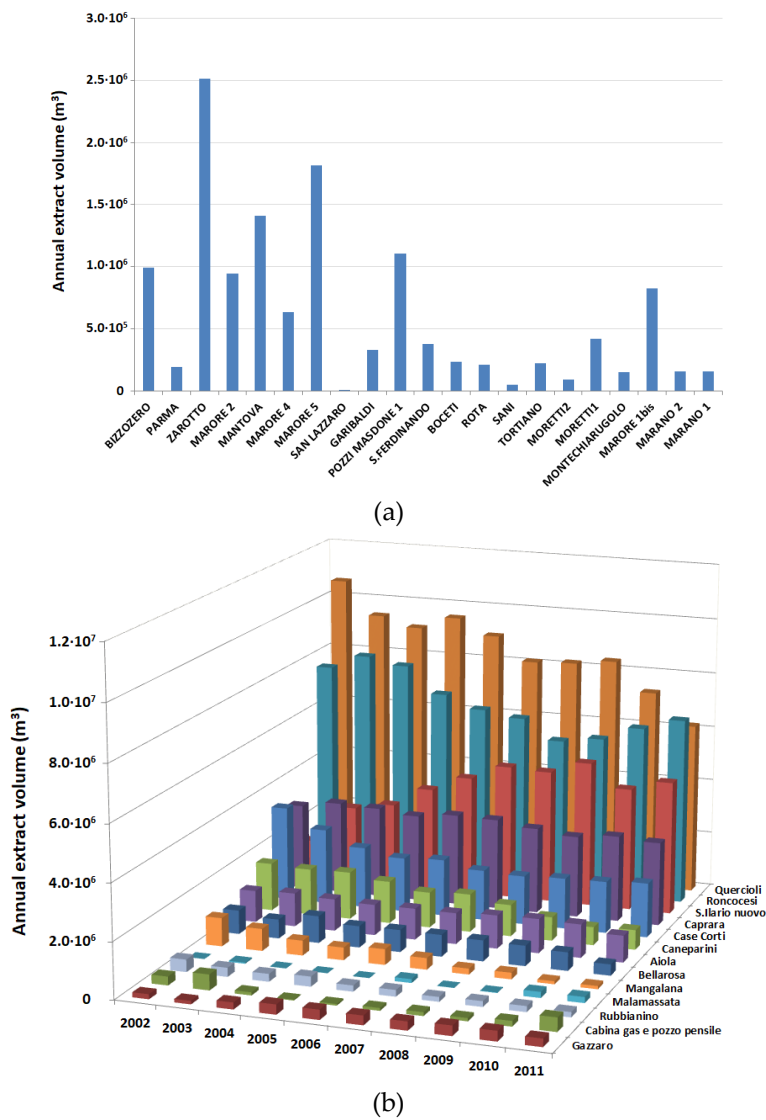
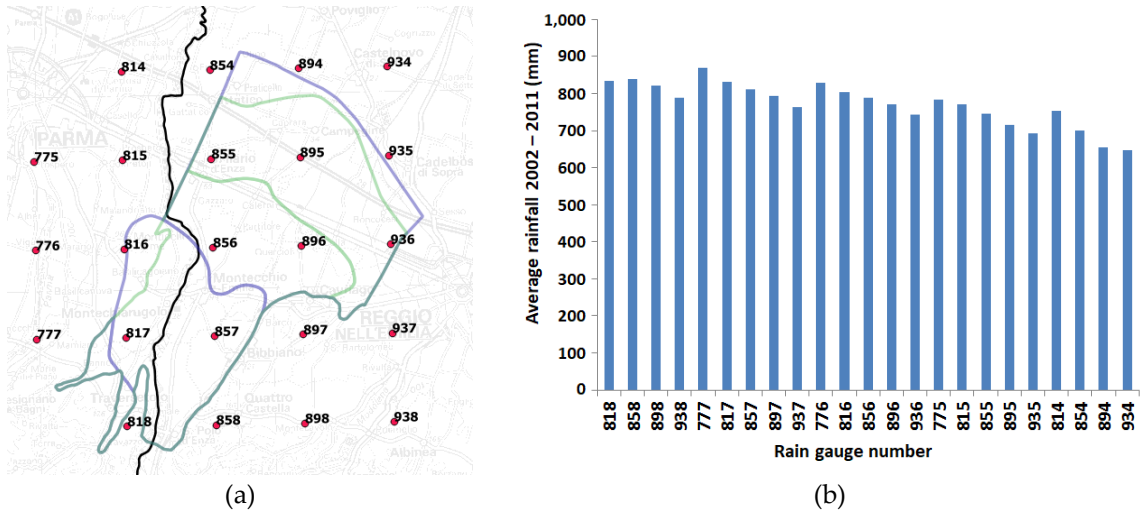
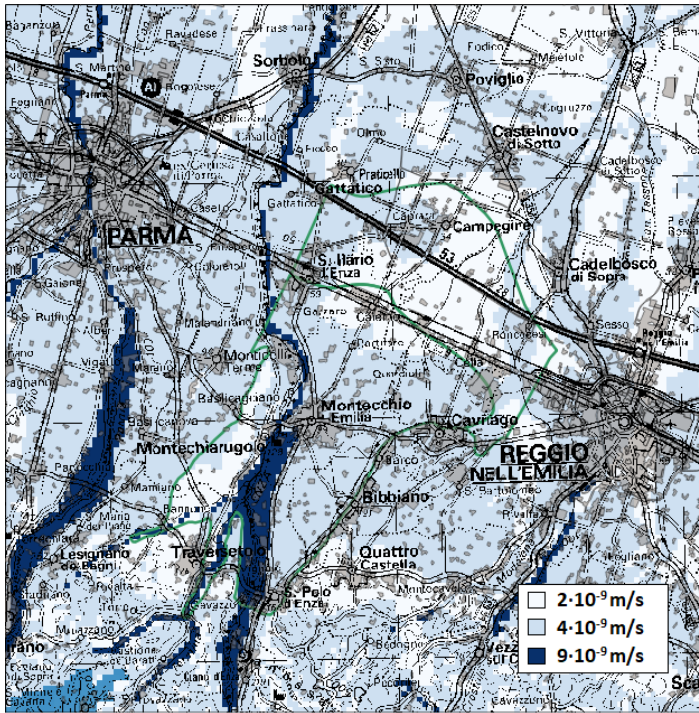


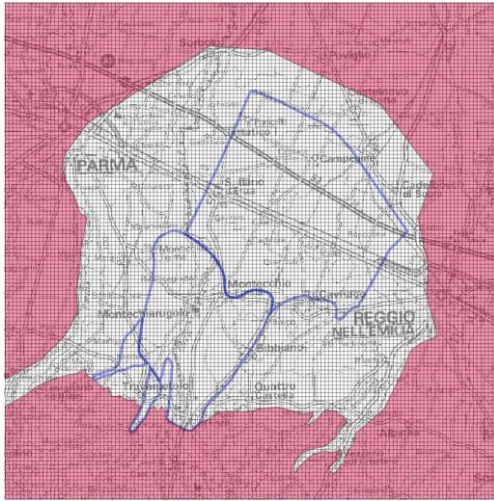
Fig. S4 (a) Annual average volume extracted from Parma wells; (b) Annual extract volume from Reggio Emilia well fields, from 2002 to 2012



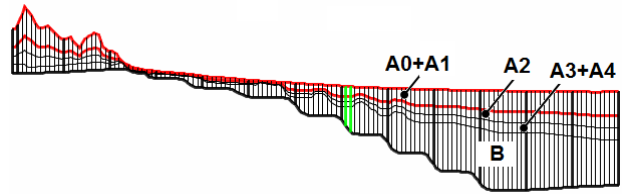
**Fig. S5** (a) Rain gauges location in the study area; (b) Average rainfall in 2002-2012 decade at each rain gauge



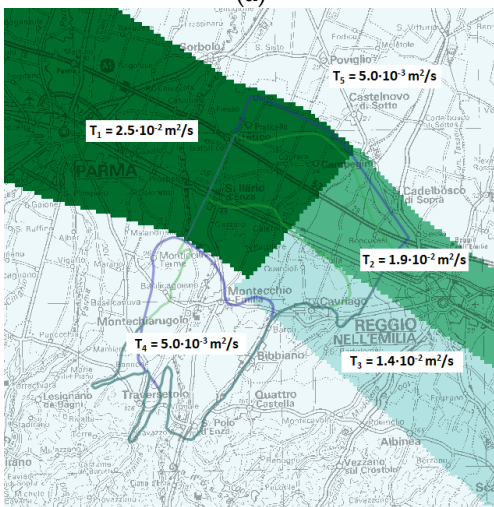
**Fig. S6** Distribution of recharge rate by soil type (urban impermeable areas in grey).



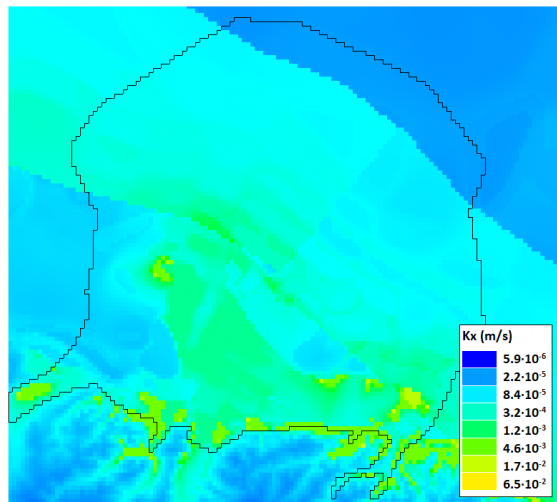
(a)



(b)

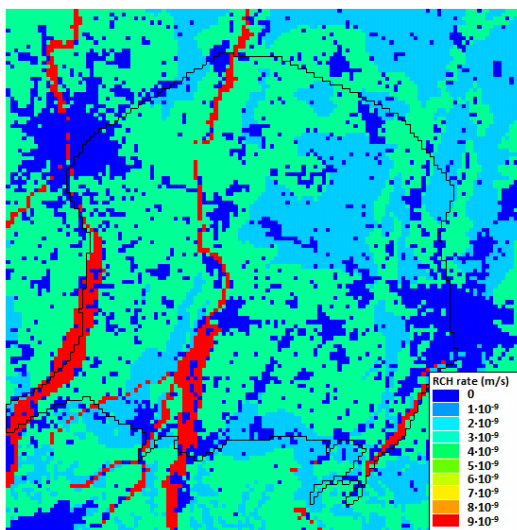


(c)

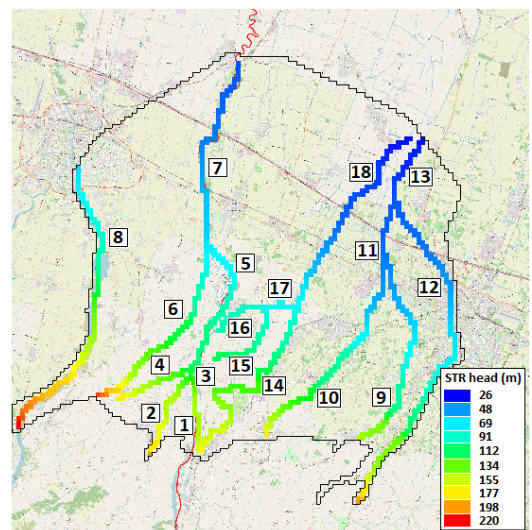


(d)

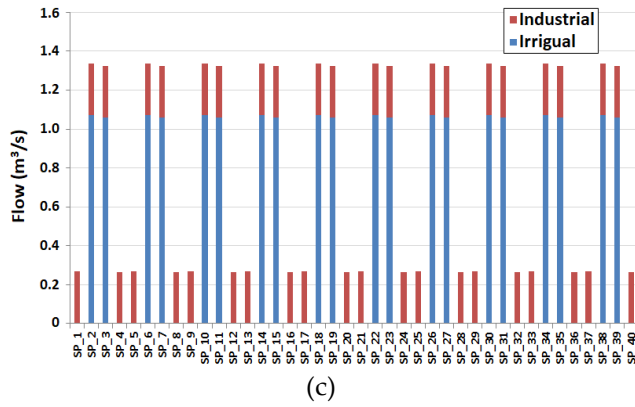
**Fig. S7** (a) Active area of the model (white area); (b) Vertical schematization of the model; (c) Transmissivity distribution ( $m^2/s$ ), for aquifer Group A; (d)  $k_{hor}$  distribution for the first three layers.



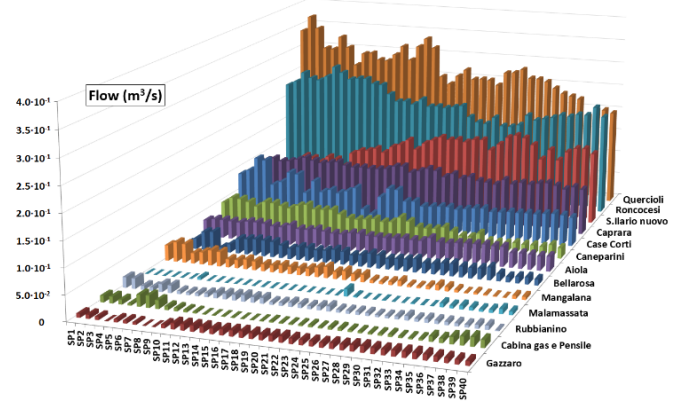
(a)



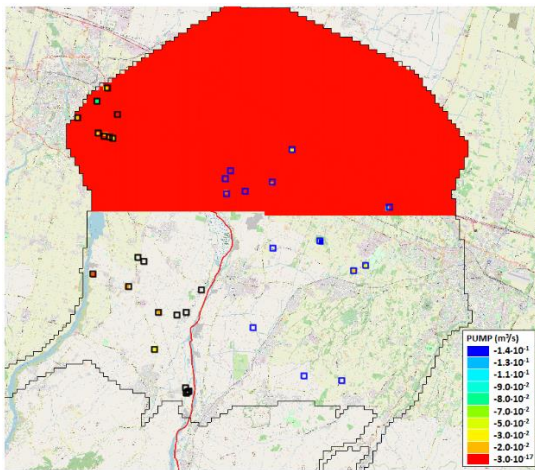
(b)



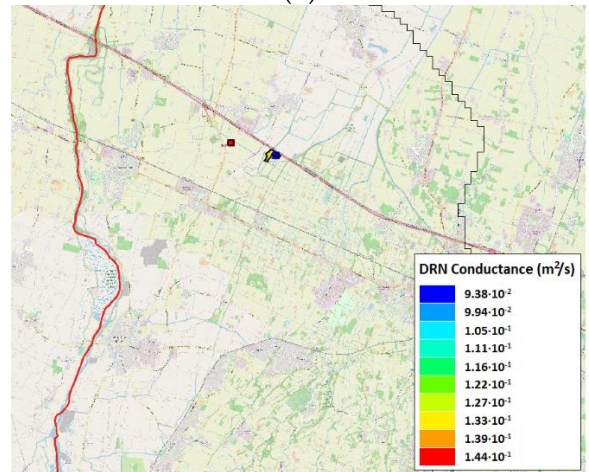
(c)



(d)

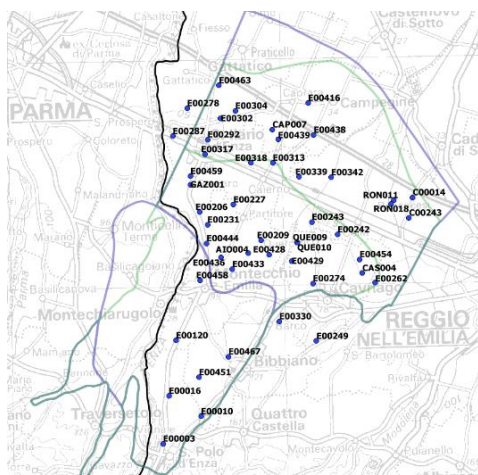


(e)

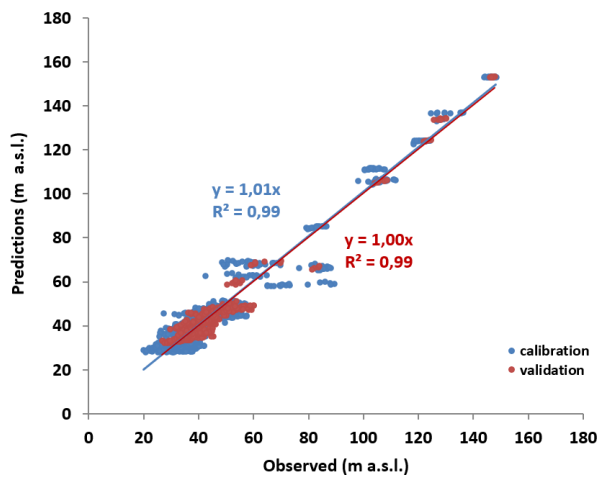


(f)

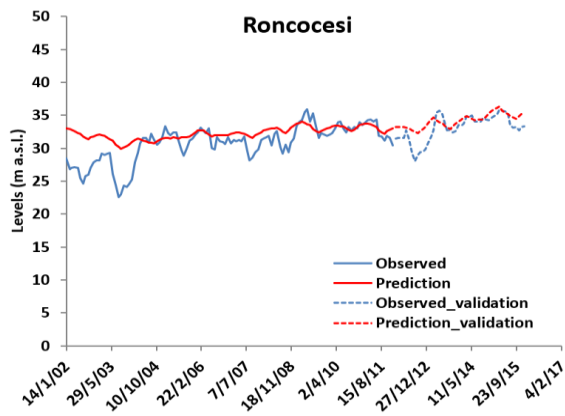
**Fig. S8** (a) Effective recharge rate; (b) Hydrographic network, with hydraulic head and hierarchy of rivers; (c) Irrigation/industrial and (d) civil withdrawals from the well fields of Reggio Emilia Province, over the 2002-2012 period; (e) Civil (blue and black squares) and irrigation/industrial (red) withdrawals; (f) “Fontanili” inserted in the model



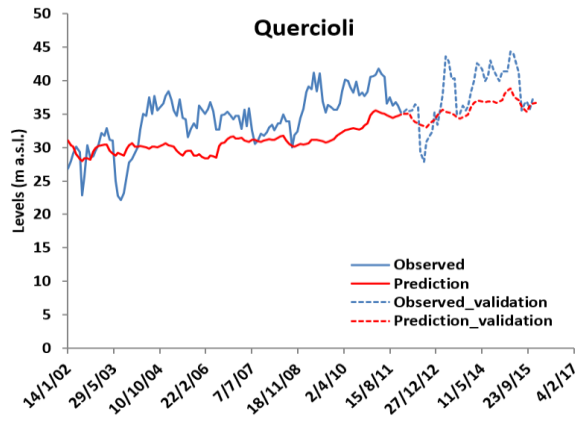
(a)



(b)



(c)



(d)

**Fig. S9** (a) Location of wells (water company and private) used for calibration and validation; (b) Observed values vs. predictions; (c) - (d) Trend of observed vs. predicted levels in calibration and validation, for Roncocesi and Quercioli wells

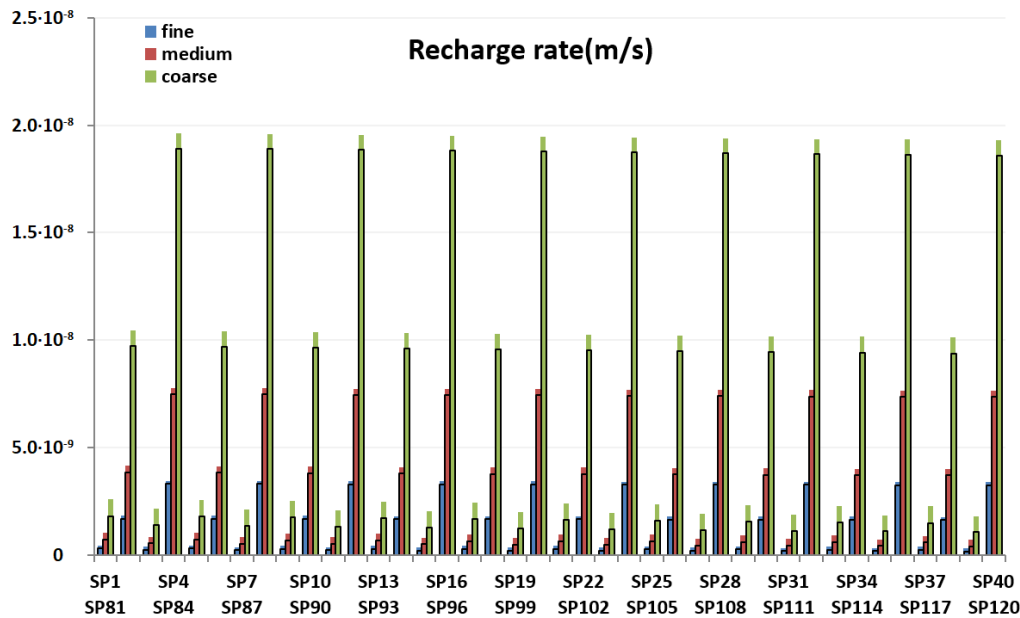


**Fig. S10** Recharge rate (m/s) for different soil types, for the first (SP1 - SP40) and last (SP81 - SP120) decade of 30-year time horizon, in ST1 model. The histogram of the decade SP81 - SP120 has black borders

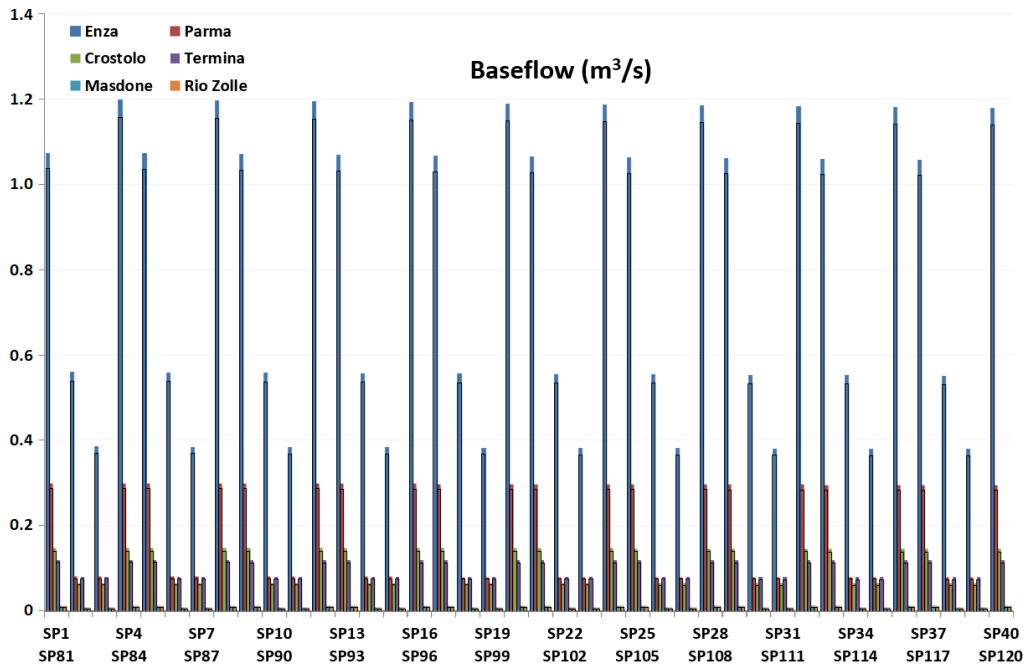
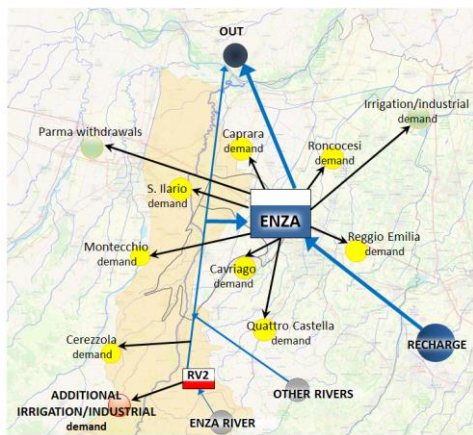
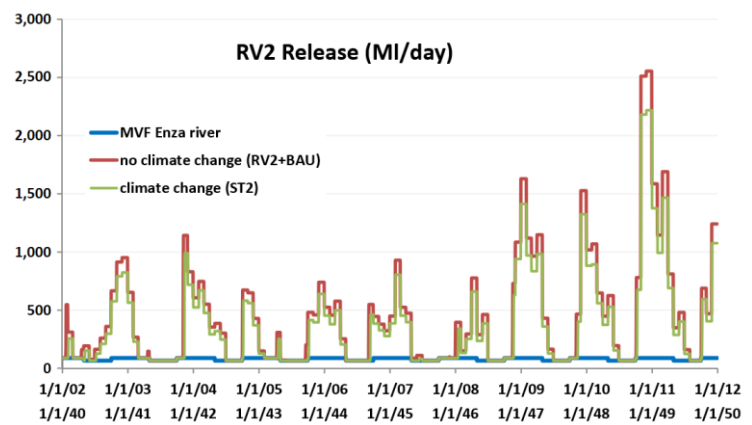


**Fig. S11** Baseflow ( $\text{m}^3/\text{s}$ ) of main rivers in the ST1 model, and for the first (SP1 - SP40) and last (SP81 - SP120) decade of 30-year time horizon. The histogram of the decade SP81 - SP120 has black borders



(a)



(b)

**Fig. S12** (a) Schematization of water supply network; (b) Release from RV2, with and without climate changes, compared with Enza's MVF.

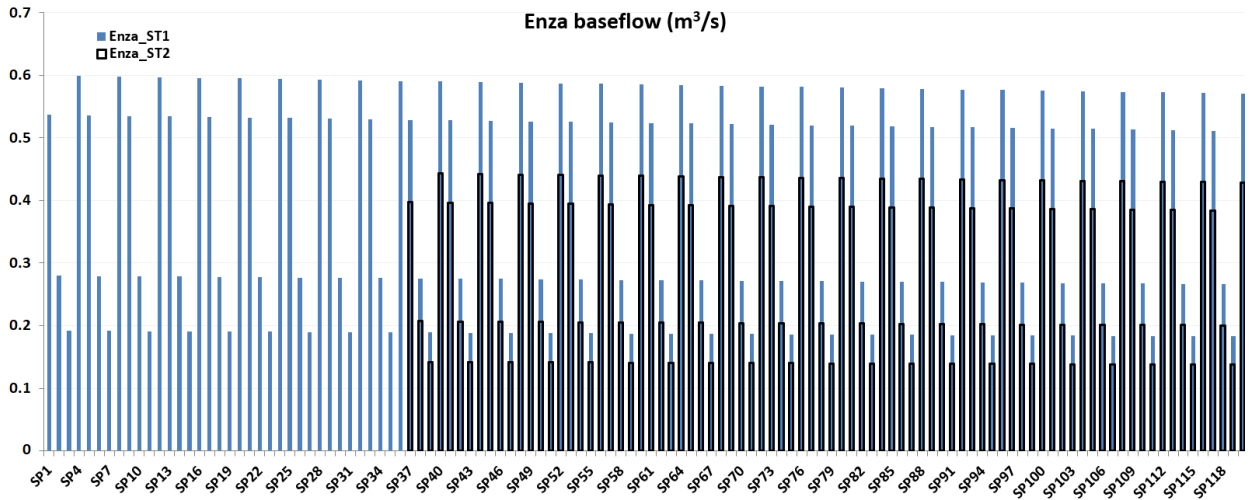


**Fig. S13** Comparison between Enza baseflow in ST1 and ST2

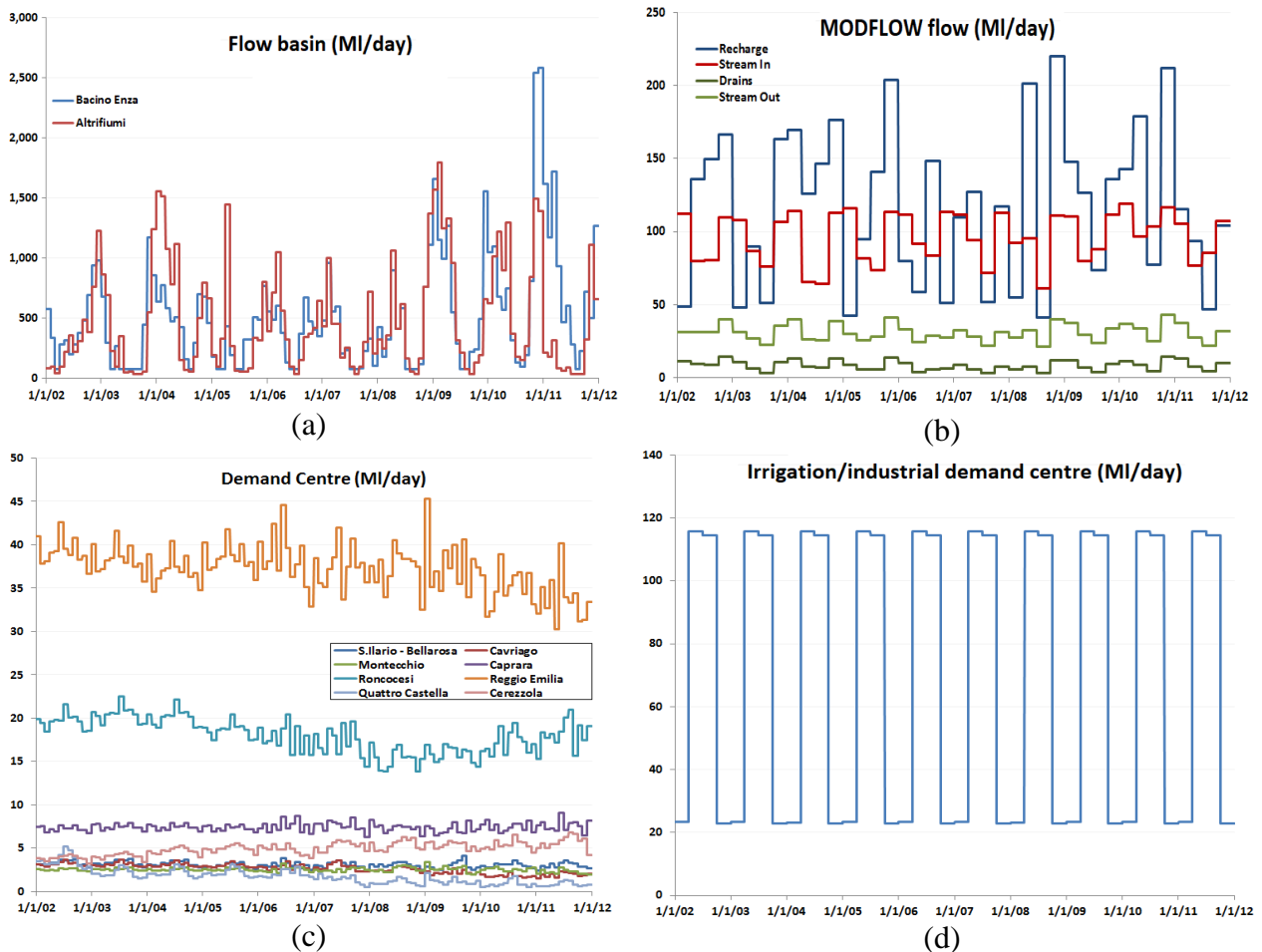


**Fig. S14** (a) Surface water flows for Enza basin and Altrifumi, in the 2002-2012 period; (b) Flow time series derived by BAU (MODFLOW); (c) Flow time series associated with the demand centers served by the well fields in of Reggio Emilia Province; (d) Time series of irrigation and industrial withdrawals.

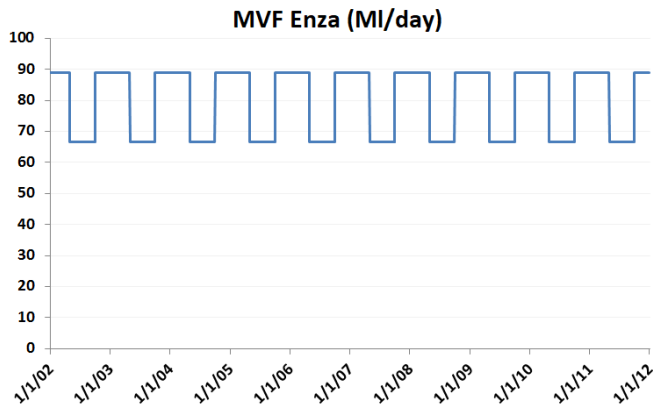
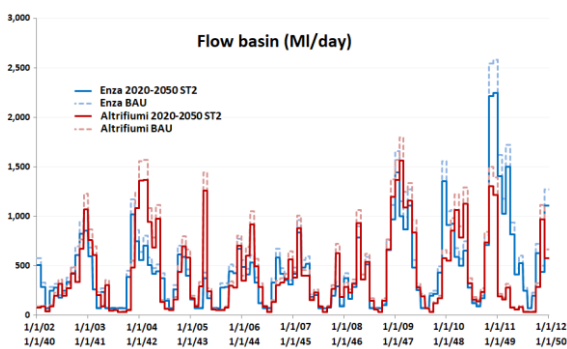
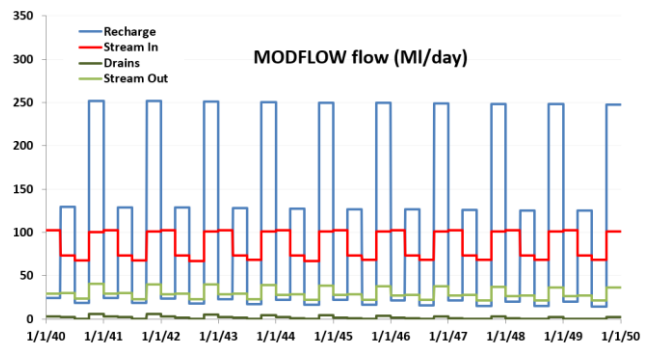


**Fig. S15** Daily time series of Enza MVF

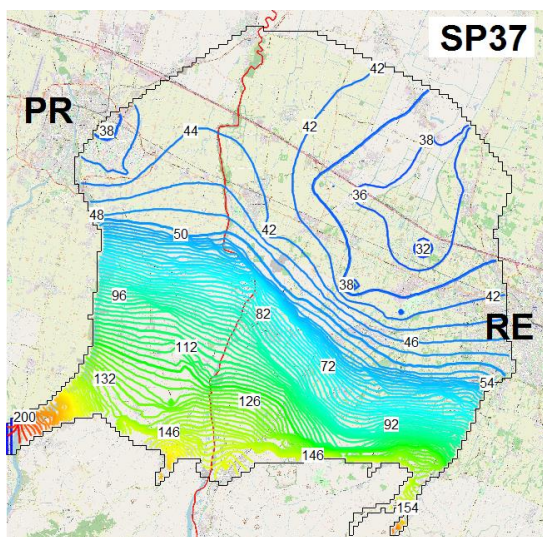


(a)

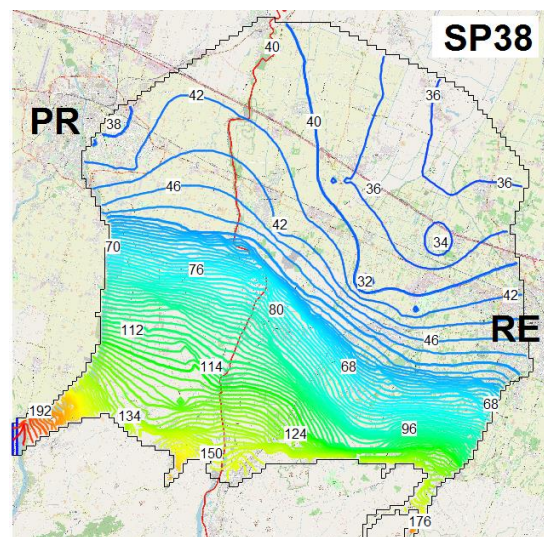


(b)

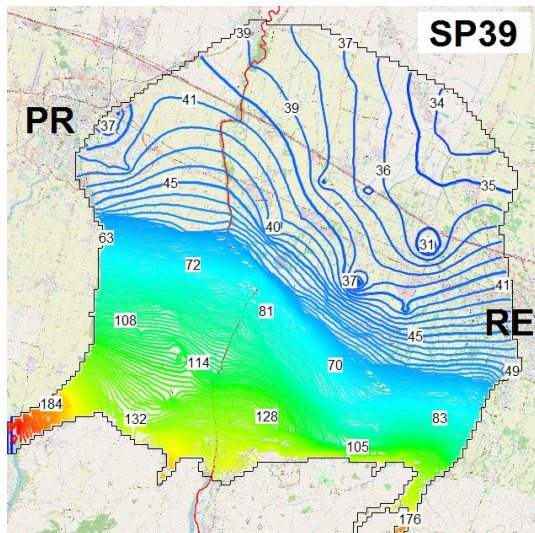
**Fig. S16** (a) Flow from Enza basin and Altrifiumi, for ST2 and BAU simulation; (b) Flow time series derived by ST2 (MODFLOW)



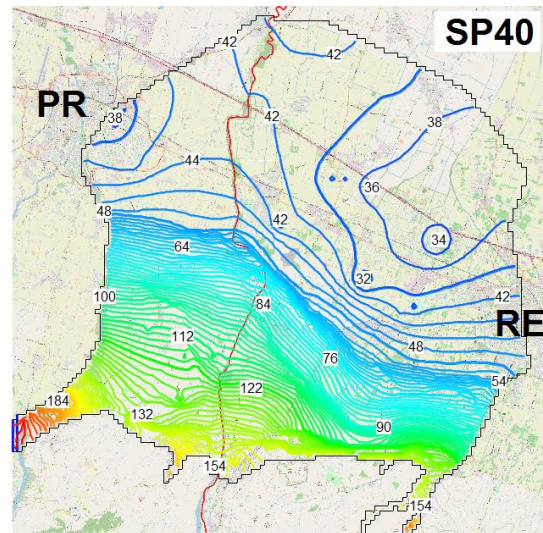
(a)



(b)

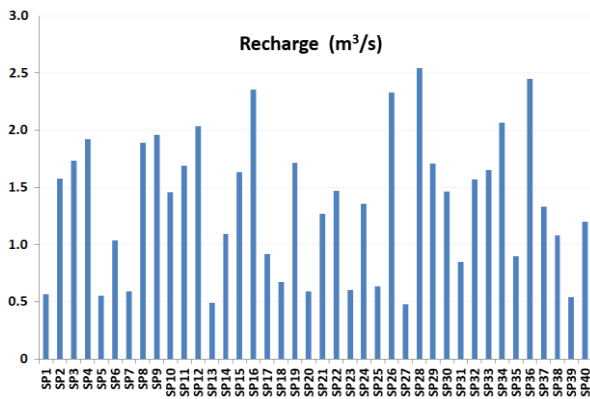


(c)

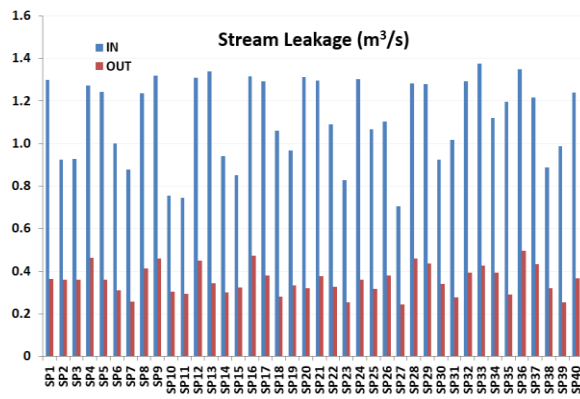


(d)

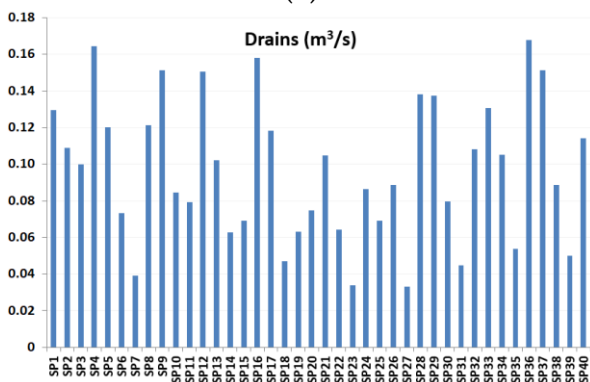
Fig. S17 (a) – (d) Hydraulic head within layer 1, BAU scenario, last year of simulation (2011)



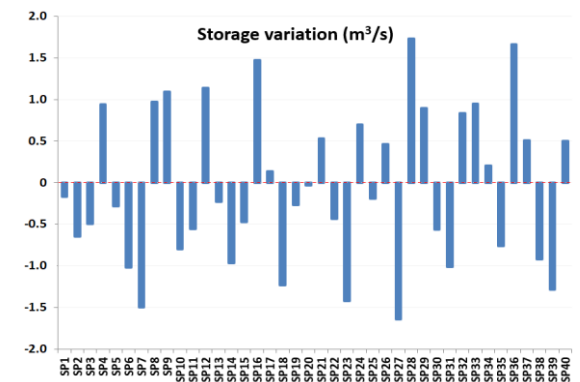
(a)



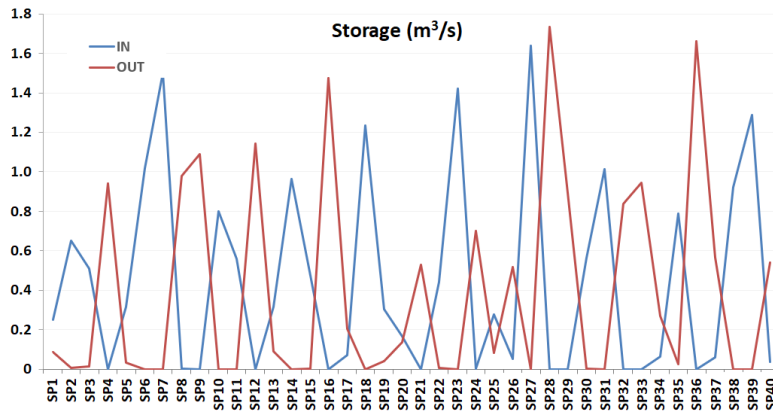
(b)



(c)

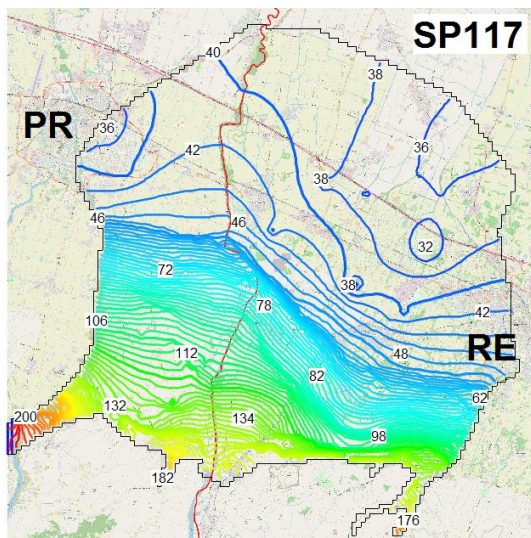


(d)

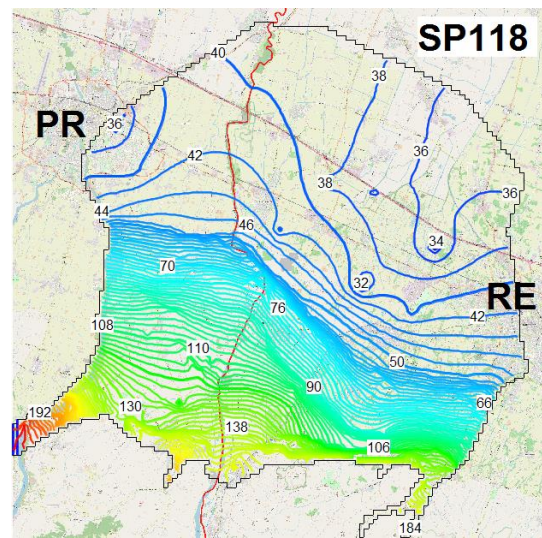


(e)

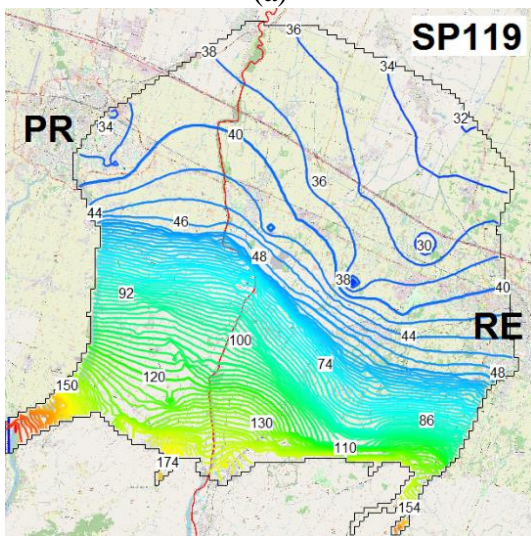
**Fig. S18** (a) – (e) Volumetric budget, derived by BAU model: Recharge, Stream leakage In/Out, Drains, Storage variation, and Storage In/Out



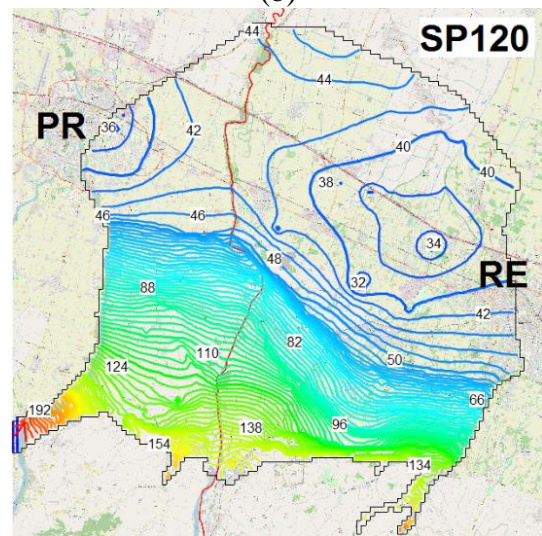
(a)



(b)



(c)



(d)

**Fig. S19** (a) – (d) Hydraulic head within layer 1, ST1 scenario, last year of simulation (2049)

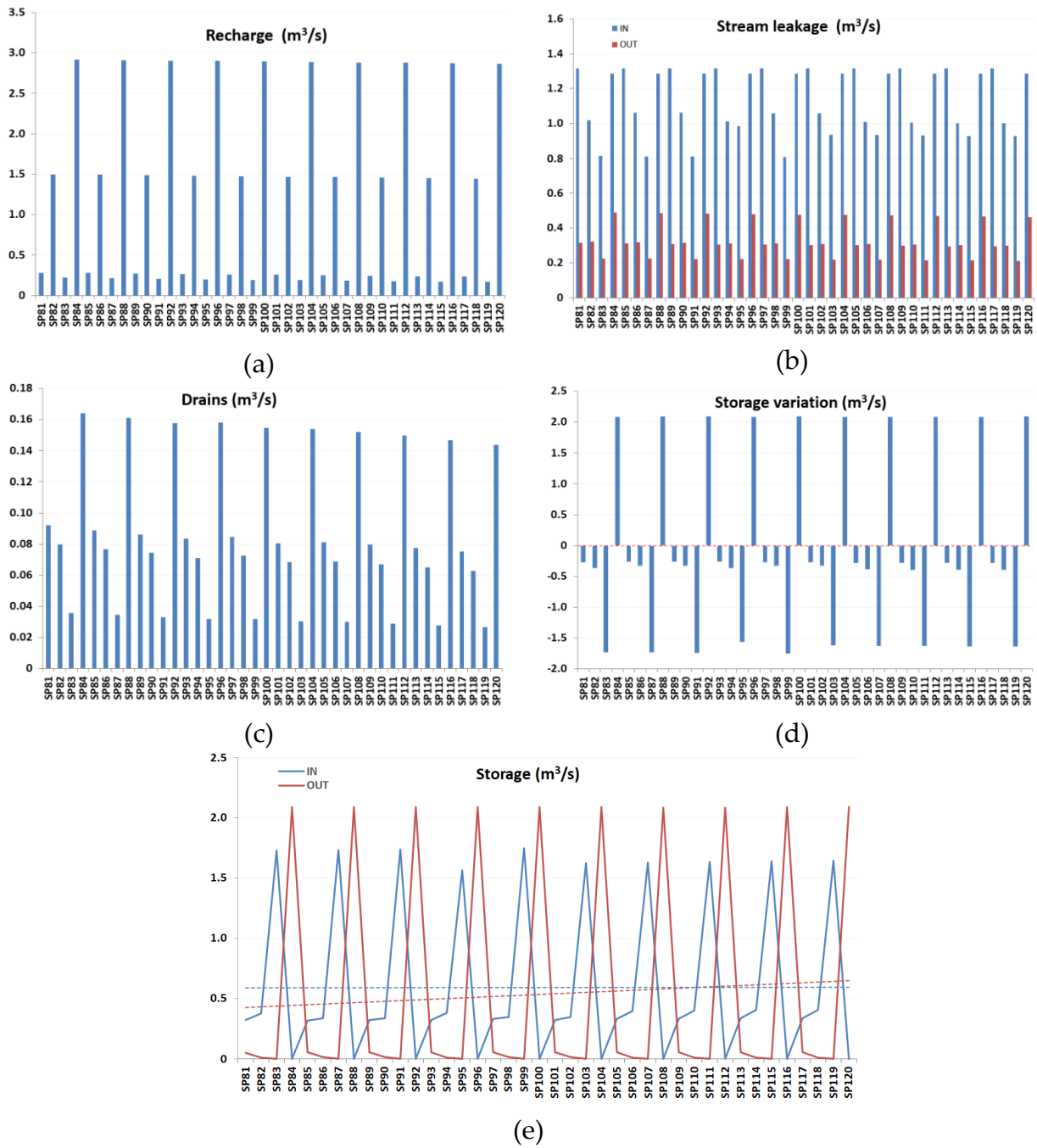
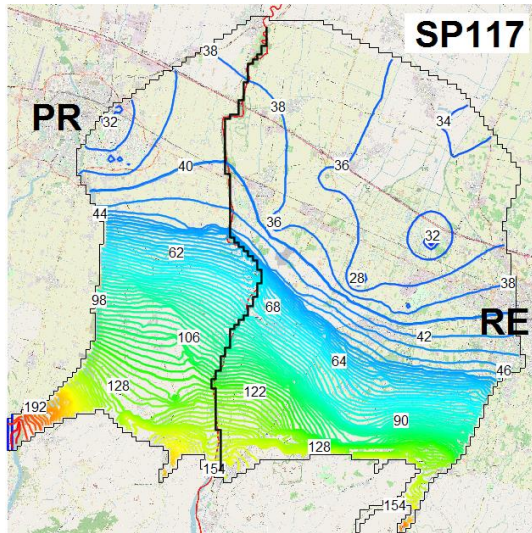
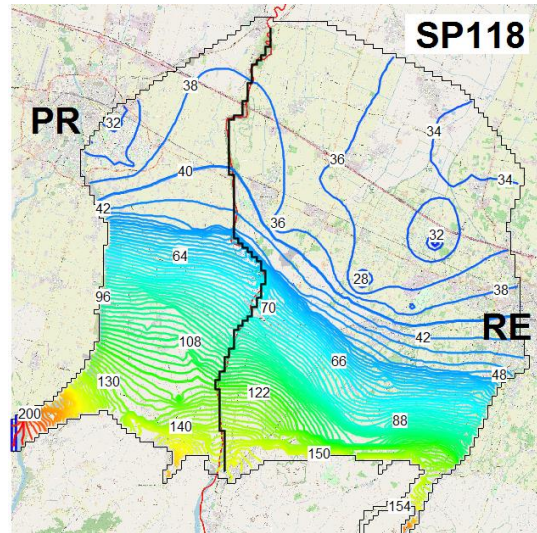


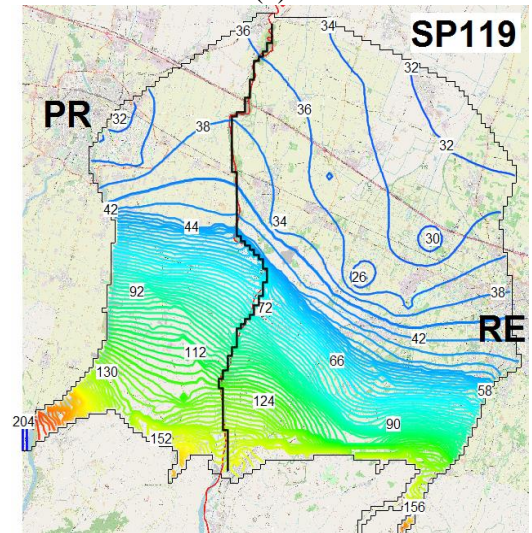
**Fig. S20** (a) – (e) Volumetric budget, derived by ST1 model: Recharge, Stream leakage In/Out, Drains, Storage variation, and Storage In/Out.



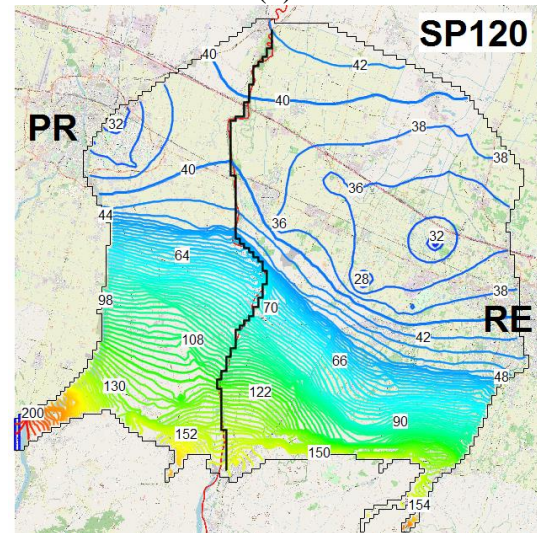
(a)



(b)

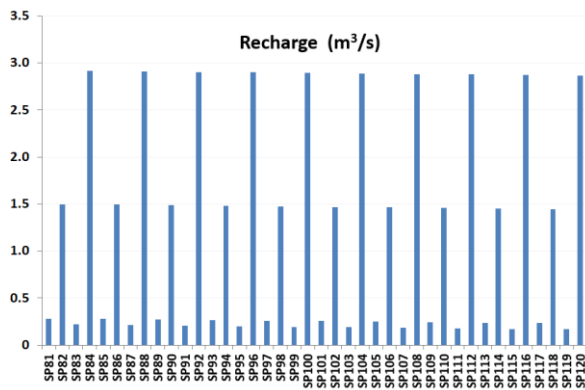


(c)

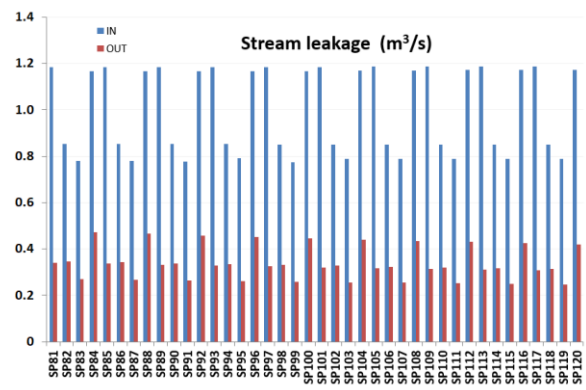


(d)

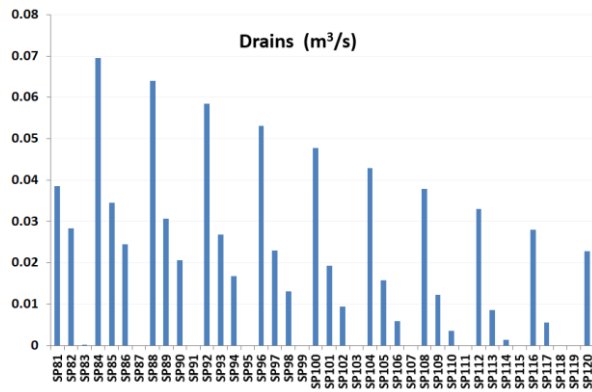
**Fig. S21** (a) – (d) Hydraulic head within layer 1, ST2 scenario, last year of simulation (2049)



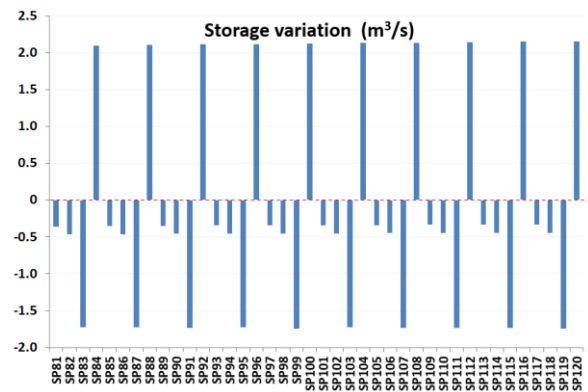
(a)



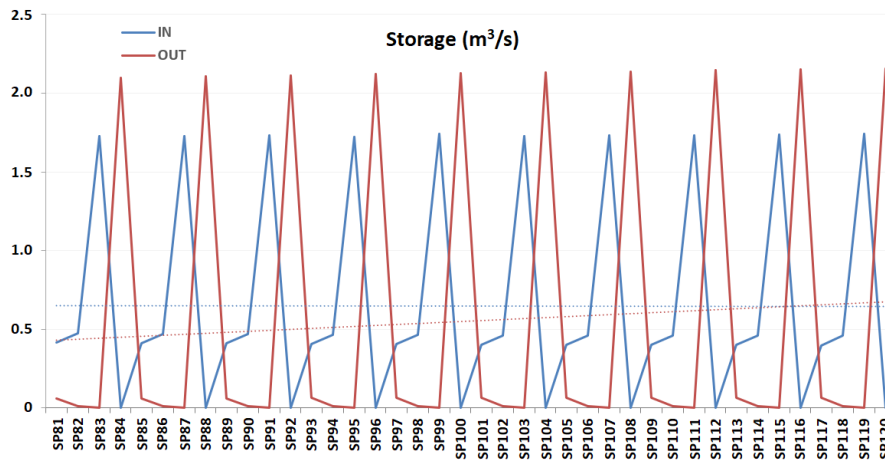
(b)



(c)



(d)



(e)

**Fig. S22** (a) – (e) Volumetric budget, derived by ST2 model: Recharge, Stream leakage In/Out, Drains, Storage variation, and Storage In/Out.

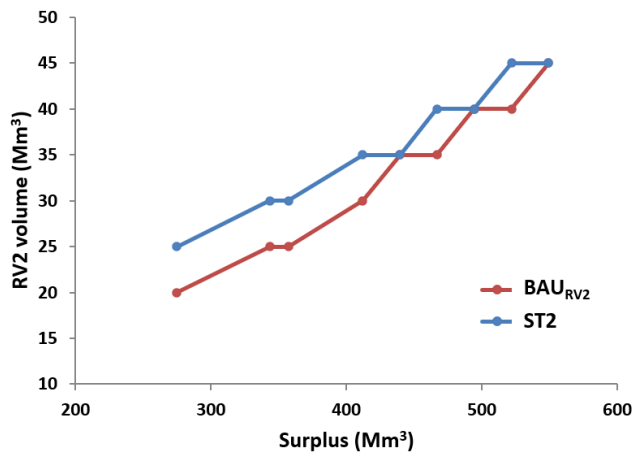
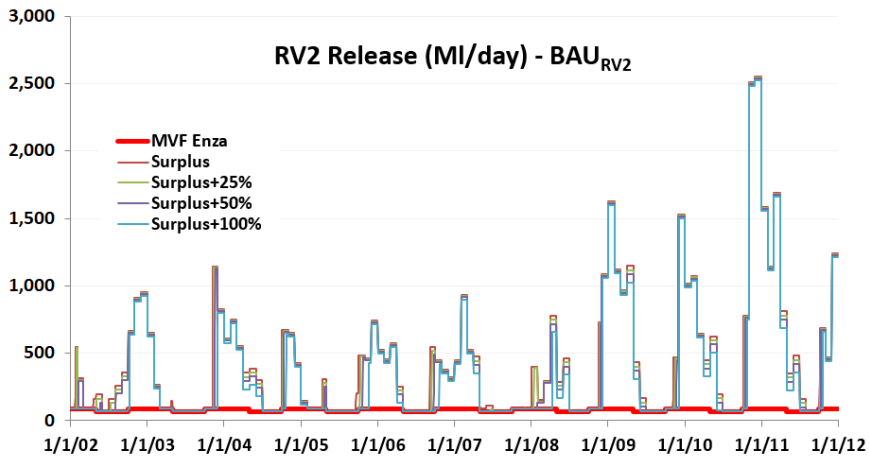
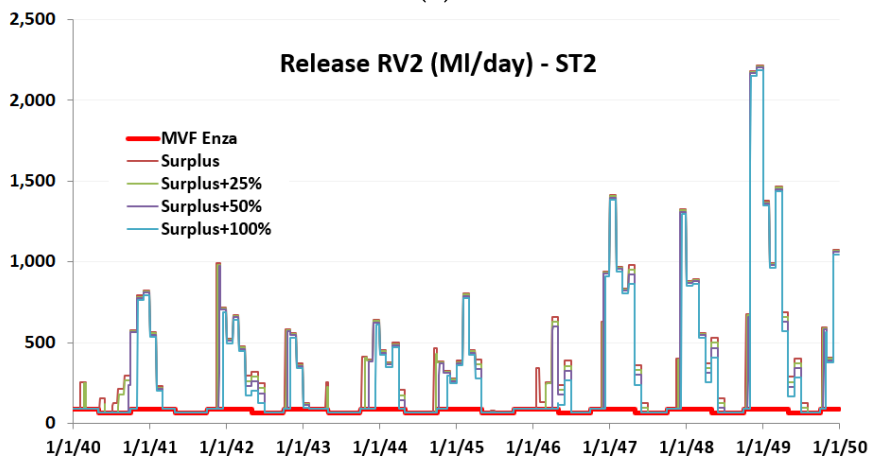


**Fig. S23** RV2 volume able to satisfy a given irrigation/industrial Surplus for Aquator scenarios BAURV2 and ST2.



(a)



(b)

**Fig. S24** Release from RV2 reservoir in scenario BAU<sub>RV2</sub> (a) and ST2 (b)

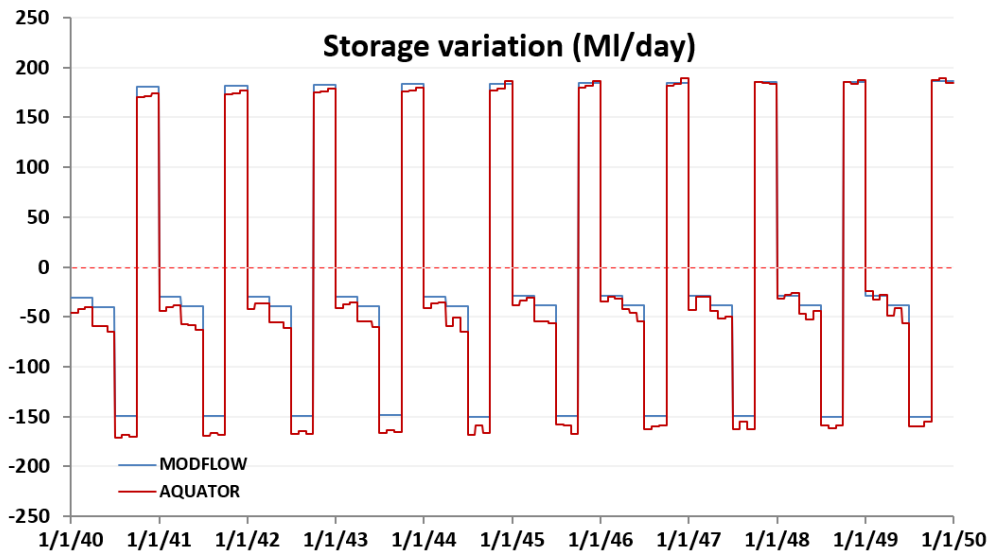


**Fig. S25** Enza storage variation in MODFLOW and Aquator models, for ST2